Controlled exchange interaction for quantum logic operations with spin qubits in coupled quantum dots

S. Moskal, S. Bednarek,* and J. Adamowski
Faculty of Physics and Applied Computer Science, AGH University of Science and Technology, Kraków, Poland
(Received 24 April 2007; published 4 September 2007)

A two-electron system confined in two coupled semiconductor quantum dots is investigated as a candidate for performing quantum logic operations with spin qubits. We study different processes of swapping the electron spins by a controlled switching on and off of the exchange interaction. The resulting spin swap corresponds to an elementary operation in quantum-information processing. We perform direct simulations of the time evolution of the two-electron system. Our results show that, in order to obtain the full interchange of spins, the exchange interaction should change smoothly in time. The presence of jumps and spikes in the time characteristics of the confinement potential leads to a considerable increase of the spin-swap time. We propose several mechanisms to modify the exchange interaction by changing the confinement potential profile and discuss their advantages and disadvantages.

DOI: 10.1103/PhysRevA.76.032302 PACS number(s): 03.67.Lx, 03.67.Mn, 73.21.La

I. INTRODUCTION

In quantum computations, one- and two-qubit logic gates play a crucial role, since they allow us to perform an arbitrary quantum logic operation [1]. Recent, practical realization of these gates has been a challenge for many physical laboratories. Among several propositions of constructing systems performing two-qubit gates, the most promising are these based on the mechanism of a controlled switching on and off of the exchange interaction between spin qubits [2–14]. Tuning the exchange interaction between electrons in coupled quantum subsystems can lead to an interchange of qubit states and, as a consequence, to the performance of a designed quantum logic operation.

A physical implementation of the controlled exchange interaction itself is a difficult task. Moreover, the elements of a future quantum computer have to fulfill several conditions, known in the form of DiVincenzo criteria [15]. One of them is a scalability, which allows one to join the elements into a computational machine. It is expected that semiconductor nanodevices, in particular those consisting of semiconductor quantum dots (QDs), should be scalable to large enough size. Recently, electron spin states have been regarded to be the most promising candidates for qubits [6,8,9,16–19] due to the long coherence time [20]. Quantum-information processing can be performed via changes of the electron spin states [8,16,17]. A spin flip can result from a precession in the external static magnetic field [14,21] or an irradiation of the electron system by an electromagnetic wave with frequency adjusted to the Zeeman splitting [5,22]. The spin swap can be caused by an exchange interaction between the two electrons [2].

Coherent control of two-electron spin states in coupled QDs has been realized by Petta *et al.* [18]. Applying the suitably chosen gate voltage pulses to the double QD, the authors [18] performed a quantum-state preparation, coherent manipulation, and projective readout of the two-spin qubits. The coherence time is limited by hyperfine interactions of the electron spin with nuclear spins of GaAs. Using quantum control techniques, Petta *et al.* [18] estimated that the coherence time for two-electron spin qubits exceeds 1 μs. Meunier *et al.* [19] performed a nondestructive measurement of two-electron spins in a single QD. This measurement allowed the authors [19] to realize a repeated identification of singlet- and triplet-electron-spin states with the same outcome every time. Therefore, this technique is very promising for the storage and processing of the quantum information.

A general theory of the two-electron spin manipulation in coupled QDs was presented, e.g., [16,17,23]. In particular, Schliemann *et al.* [17] considered a coupled QD system with the tunneling matrix element approximated by a smooth function of time, which led them to the conclusion that the swap of electron spins can be unperturbed by a possible double occupancy of the QD.

In the present paper, we study the swap operation of the two-electron spins, which results from a controlled switching on and off of the exchange interaction between the electrons in coupled QDs. The exchange interaction is switched on and off as a result of designed time changes of the QD confinement potential. We propose different schedules of changing the confinement potential, which are described by smooth as well as non smooth time characteristics. We show that these time characteristics are of crucial importance for the resulting spin swap; in particular, the non smooth time dependence of the QD confinement potential can lead to a non adiabatic spin-swap process with ill-defined spins of the electrons.

A properly tuned exchange interaction leads to a swapping of electron spins [2,3,9,14,16,24]. We describe this process for a two-electron system in coupled QDs using a model that takes into account all three space dimensions, electron spins, and interelectron interactions, but neglects electron spin-nuclear spin interactions [25]. We apply the adiabatic approximation in order to decouple the transverse and longitudinal degrees of freedom and perform an integration over the transverse spatial coordinates. This leads to the effectively one-dimensional two-electron problem [26], which can be solved by the numerical method with an arbitrary preci-

*bednarek@novell.ftj.agh.edu.pl

sion [27]. The system under study is described by the two-particle wave function of the form of a four-component state vector, which takes into account all possible spin configurations. We consider different methods of turning on and off the exchange interaction between the electrons and investigate the resulting changes of electron spins. The present computer simulations are based on accurate numerical solutions of the time-dependent Schrödinger equation; i.e., they allow us to trace the time evolution of the electron system in a direct manner. Therefore, the present results fill in a gap between quantum-information theory and experiment. We hope that these results will serve as a guide for experimental groups, which are involved in designing and constructing the nanodevices with spin qubits.

The paper is organized as follows: the theoretical model is presented in Sec. II, the numerical method is described in Sec. III, and the results are presented in Sec. IV (for the vertically coupled QDs) and in Sec. V (for the laterally coupled QDs). Section VI contains a discussion and Sec. VII conclusions and summary.

II. THEORETICAL MODEL

The present paper is based on a model proposed by the present authors in Ref. [28]. We extend the model of Ref. [28] by taking explicitly into account the spin states of electrons. For the sake of completeness, below we repeat the major steps of the approach [28]. We study two electrons localized in a double-QD nanostructure. We assume a cylindrical symmetry of the system with the symmetry axis (z axis) going through the geometrical centers of the QDs. The potential confining the electrons in the x-y plane is taken to be sufficiently strong that the differences between the energy levels resulting from the x-y space quantization are much larger than the electron-electron interaction energy. This potential is usually called the lateral confinement potential. We approximate the lateral potential by the two-dimensional harmonic oscillator potential and assume that both electrons occupy the ground state in the x-y motion. In other words, we assume that the lateral (transverse) electron degrees of freedom are frozen. The above assumptions allow us to reduce the starting three-dimensional problem to the effectively one-dimensional problem [26] with the electron-electron interaction being the following function of z_1 and z_2 coordinates of both the electrons:

$$V_{eff}(z_1,z_2) = \frac{e^2\sqrt{\pi\beta}}{4\pi\varepsilon_0\varepsilon} e^{\beta|z_1-z_2|^2}\,\mathrm{erfc}(\sqrt{\beta}|z_1-z_2|), \qquad (1)$$

where ε_0 is the vacuum electric permittivity, ε is the static electric permittivity, $\beta=m_e\omega_\perp/(2\hbar)$, m_e is the electron effective conduction band mass, and $\hbar\omega_\perp$ is the excitation energy of the electron transverse motion. The Hamiltonian of the system takes the form [26]

$$H = -\frac{\hbar^2}{2m_e}\left(\frac{\partial^2}{\partial z_1^2}+\frac{\partial^2}{\partial z_2^2}\right) + V(z_1,t) + V(z_2,t) + V_{eff}(z_1,z_2), \qquad (2)$$

where $V(z_i,t)$ is the potential energy of the vertical confinement of the ith electron. In the following, vertical confinement energy $V(z,t)$ will be in general taken in a form of two potential wells separated by the potential barrier. In Eq. (2), we have omitted the constant $2\hbar\omega_\perp$—i.e., the excitation energy of the transverse motion of two electrons. In the calculations, we take on the parameters which correspond to nanostructure based on GaAs: $m_e=0.067m_{e0}$, where m_{e0} is the free-electron rest mass and the static electric permittivity $\varepsilon=11.0$.

In the two-electron system, we are dealing with four independent spin states; therefore, the total wave function of the system can be represented by the following four-component vector:

$$\Psi(z_1,z_2) = \begin{pmatrix} \psi_{\uparrow\uparrow} \\ \psi_{\uparrow\downarrow} \\ \psi_{\downarrow\uparrow} \\ \psi_{\downarrow\downarrow} \end{pmatrix}, \qquad (3)$$

where $\psi_{nm}=\psi_{nm}(z_1,z_2)$ are the basis wave functions with indices $n,m=\uparrow,\downarrow$, which correspond to the z-spin component eigenvalues $\pm\hbar/2$, respectively. The basis wave functions ψ_{nm} do not possess well-defined symmetry. However, the total wave function (3) has to be antisymmetric with respect to simultaneous exchange of the space and spin coordinates. This property imposes the following conditions on the basis wave functions:

$$\psi_{\uparrow\uparrow}(z_1,z_2) = -\psi_{\uparrow\uparrow}(z_2,z_1), \qquad (4a)$$

$$\psi_{\downarrow\uparrow}(z_1,z_2) = -\psi_{\uparrow\downarrow}(z_2,z_1), \qquad (4b)$$

$$\psi_{\downarrow\downarrow}(z_1,z_2) = -\psi_{\downarrow\downarrow}(z_2,z_1). \qquad (4c)$$

In representation (3), the operators of the total spin are expressed by the following 4×4 matrices:

$$\sigma_x^{tot} = \begin{pmatrix} \sigma_x & \mathbb{1} \\ \mathbb{1} & \sigma_x \end{pmatrix}, \quad \sigma_y^{tot} = \begin{pmatrix} \sigma_y & -i\mathbb{1} \\ i\mathbb{1} & \sigma_y \end{pmatrix}, \qquad (5)$$

$$\sigma_z^{tot} = \begin{pmatrix} \sigma_z+\mathbb{1} & 0 \\ 0 & \sigma_z-\mathbb{1} \end{pmatrix},$$

where $\mathbb{1}$ denotes the unit 2×2 matrix and σ_x, σ_y, and σ_z are the spin Pauli matrices. The corresponding expectation values are calculated as $\langle\sigma_k^{tot}\rangle=\langle\Psi|\sigma_k^{tot}|\Psi\rangle$, where $k=x,y,z$. The expectation values of the total spin components are obtained from $S_k^{tot}=(\hbar/2)\langle\sigma_k^{tot}\rangle$.

Due to their indistinguishability, the electrons cannot be numerated, therefore, we can not determine which electron is in a given spin state. However, we can distinguish the two quantum dots, determined by the corresponding potential wells. We shall call them the left and right QDs (potential wells). If both QDs are separated by the nonpenetrable potential barrier, which does not allow for a tunneling of electrons, then, in the ground state of the system, each electron is localized in a single QD. Owing to this, we can determine the spins of electrons in the left and right QDs. For this purpose, we introduce the auxiliary wave function $\varphi(z_1,z_2)$, which will be called the reference wave function. This wave

function is a solution of the Schrödinger equation for the two distinguishable particles, which, with an exception of indistinguishability, possess all the properties of the electrons. For the distinguishable particles we do no perform a symmetrization of the two-particle wave function. Instead the solutions found for $\varphi(z_1,z_2)$ correspond to the configuration, in which one electron (described by coordinate z_1) is localized in the left QD and the other (z_2) is in the right QD. This state always exists if the tunneling through the barrier is not possible. In each simulation performed, these configurations are realized at the initial ($t=0$) and final ($t=T$) time instants. The reference wave function will serve to a construction of the initial state wave function and a determination of the spin states of electrons in both the QDs. The expectation values of spin components are calculated as follows:

$$S_k^j = \frac{\hbar}{2}\langle\sigma_k^j\rangle = \frac{\hbar}{2}u^T\sigma_k^j u, \tag{6}$$

where $j=L,R$ corresponds to the electron localized in the left (L) and right (R) QD, and

$$u = \begin{pmatrix} \langle\varphi|\psi_{\uparrow\uparrow}\rangle \\ \langle\varphi|\psi_{\uparrow\downarrow}\rangle \\ \langle\varphi|\psi_{\downarrow\uparrow}\rangle \\ \langle\varphi|\psi_{\downarrow\downarrow}\rangle \end{pmatrix}. \tag{7}$$

The spin matrix operators in Eq. (6) have the form

$$\sigma_x^L = \begin{pmatrix} 0 & 1 \\ 1 & 0 \end{pmatrix}, \quad \sigma_y^L = i\begin{pmatrix} 0 & -1 \\ 1 & 0 \end{pmatrix}, \quad \sigma_z^L = \begin{pmatrix} 1 & 0 \\ 0 & -1 \end{pmatrix}, \tag{8a}$$

$$\sigma_x^R = \begin{pmatrix} \sigma_x & 0 \\ 0 & \sigma_x \end{pmatrix}, \quad \sigma_y^R = \begin{pmatrix} \sigma_y & 0 \\ 0 & \sigma_y \end{pmatrix}, \quad \sigma_z^R = \begin{pmatrix} \sigma_z & 0 \\ 0 & \sigma_z \end{pmatrix}. \tag{8b}$$

The operator of the kth component of the total spin is defined as $S_k^{tot}=(\hbar/2)(\sigma_k^L+\sigma_k^R)$.

III. SETTING UP THE COMPUTER EXPERIMENT

We simulate the process of swapping the spins for two electrons localized in two QDs, which are initially separated by the potential barrier. We consider both the vertical and lateral geometries of the QD nanostructure. In the process studied, the spins of the electrons localized in the left or right QD are flipped as a result of the controlled switching of the exchange interaction between the electrons, which leads to the spin-swap operation. We discuss two methods to control the exchange interaction. According to the first method, the exchange interaction is switched on (off) by lowering (raising) the potential barrier. During this process the inversion symmetry of the double-QD confinement potential is conserved. The second method a based on a change of the depth of one of the potential wells, which leads to a flow of electrons and their localization in the same QD. In this process, the confinement potential becomes asymmetric with respect to the inversion. In QD-based nanodevices, both methods can be implemented by changing the external voltages applied to the electrodes, which are sources of the electrostatic field forming the coupled QDs [13], or by locating the QD system in the electromagnetic field [7].

Based on an analogy with Rabi oscillations in a two-level quantum system, the process of switching on and off the exchange interaction, which leads a the change of the initial spin orientation to the opposite one, will be called the π pulse. In electrostatic QDs, the π pulse can be realized by a proper change of gate voltages. We denote the time needed to complete the spin-swap operation by T^π. We shall also deal with processes after which the expectation value of the z th component of the electron spin does not reach $\pm\hbar/2$—i.e., $|\langle S_z^j\rangle| < \hbar/2$. In such processes, the change of spin orientation is not complete.

The additional purpose of the present study is the optimization of nanodevice parameters and time changes of the confinement potential in order to make the spin-swap time possibly short. Minimization of T^π is important since this time interval determines the duration of the elementary quantum logic operation that should be much shorter than the coherence time of spin qubits. It is required [15] that the ratio of the gate operation time to the coherence time should be less than 10^{-4} in order to complete a computation along with several error correction runs [29] before the decoherence destroys the information stored in the qubits. In GaAs, the spin coherence time has been estimated to be longer than 1 ms [30].

At the initial time instant, the potential barrier between the left and right QDs is set to be nonpenetrable for the electrons. In each simulated process, the initial two-electron state is always prepared as the lowest-energy state, in which the electron localized in the left [right] QD possesses the spin z component $S_z^L(t=0)=+\hbar/2[S_z^R(t=0)=-\hbar/2]$. For the nonpenetrable barrier the singlet and triplet states are degenerate; i.e., the initial state is a linear combination of the singlet state and one of the triplet states (that with the total-spin z component equal to zero). The two-electron wave function that satisfies these initial conditions has the form

$$\Psi_{initial} \equiv \Psi(z_1,z_2,t=0) = \begin{pmatrix} 0 \\ \varphi(z_1,z_2) \\ -\varphi(z_2,z_1) \\ 0 \end{pmatrix}, \tag{9}$$

where $\varphi(z_1,z_2)$ is the reference wave function defined in Sec. II. Wave function (9) fulfills symmetry constraints (4). After a normalization, the wave function (9) is subjected to a temporal evolution according to the time-dependent Schrödinger equation

$$i\hbar\frac{\partial\Psi(z_1,z_2,t)}{\partial t} = H\Psi(z_1,z_2,t), \tag{10}$$

where H is given by Eq. (2) and the time dependence of potentials $V(z_i,t)$ and $V_{eff}(z_1,z_2)$ will be determined in the following sections.

The spin expectation values are calculated using Eq. (6) as follows. First, the reference wave function $\varphi(z_1,z_2)$ is calculated by the imaginary time step method [27]. The reference wave function is next applied to construct the total wave function [Eq. (9)] for $t=0$. Wave function (9) is used as the initial condition to perform the time simulation of Schrödinger equation (10). In the last step, we apply $\varphi(z_1,z_2)$ to calculate u [Eq. (7)] and S_k^l [Eq. (6)].

The results of simulations are presented as a function of duration time T of the process of switching on and off the exchange interaction. We note that we are dealing with two time intervals T and T^π, which have a different meanings. Time interval T determines the duration of the arbitrary process of changing the confinement potential. Time interval T^π determines the duration of the process during which the spins are fully swapped. At the end of each simulation, we record the expectation values of z spin component of the electron in the left (L) and right (R) QD. These final values of spins are denoted by $S_f^{L,R}$, where $S_f^{L,R}=S^{L,R}(t=T)$. Moreover, we record the energy difference $\Delta E_{fi}=E_f-E_i$ between the energies of the final (E_f) and initial (E_i) states of the system. The nonzero value of ΔE_{fi} means that the process in non adiabatic.

The numerical procedure applied allows us to detect the spins of single electrons in another manner. Namely, we can directly observe the temporal evolution of the second ($\psi_{\uparrow\downarrow}$) and third ($\psi_{\downarrow\uparrow}$) components of the total wave function [Eq. (3)]. We note that, due to the symmetry, it is sufficient to determine only one of these components, which allows us to speed up the computations. The full spin swap corresponds to the interchange of these two components—i.e.,

$$\begin{pmatrix} 0 \\ \psi_{\uparrow\downarrow} \\ \psi_{\downarrow\uparrow} \\ 0 \end{pmatrix} \leftrightarrow \begin{pmatrix} 0 \\ \psi_{\downarrow\uparrow} \\ \psi_{\uparrow\downarrow} \\ 0 \end{pmatrix}. \tag{11}$$

IV. VERTICALLY COUPLED QUANTUM DOTS

Vertically coupled QDs [31] can be described by a simple model with two rectangular potential wells separated by a rectangular barrier (Fig. 1). The vertical QDs, studied in Refs. [31,32], were fabricated on the basis of GaAs/(In,Ga)As/(Al,Ga)As heterostructure. In this section, we apply the model described in Sec. II with confinement potential energy $V(z,t)$ taken in the form of a double rectangular potential well (Fig. 1) with potential barrier energy $V_B(t)\equiv V(z=0,t)$ (Fig. 2). The exchange interaction is switched on by lowering the height of the potential barrier to the potential-well bottom level and is switched off by raising the potential barrier to the initial height. The time characteristics of the process of changing the potential barrier can be chosen in many ways. In the present paper, we have chosen the time characteristics parametrized as step, piece wise linear, and smooth functions (Fig. 2).

We choose such values of the nanostructure parameters (Fig. 1) that the electron tunneling is negligibly small at the initial and final time instants. Then, the electrons are well separated in space and one of them is localized in the left QD, while the second electron is localized in the right QD. Owing to this, the spin states of both electrons can be exactly determined in the initial as well as final time instant. We choose the same widths of the potential wells and potential barrier $d_L=d_R=d_B=10$ nm and the potential well depth $V_L=V_R=-150$ meV. At the initial time, we take the barrier top energy $V_B(0)=0$. We note that the conduction-band bottom of the barrier material is chosen as the reference energy and set equal to zero.

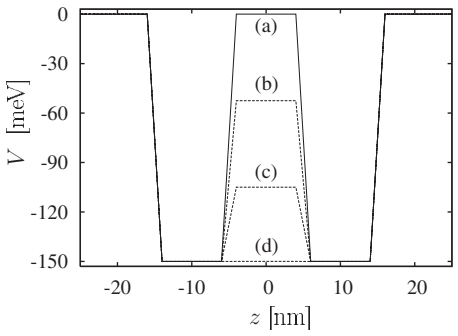

FIG. 1. Confinement potential profile V as a function of vertical coordinate z. The curves correspond to the barrier top energy V_B (a) $V_B=0$, (b) $V_B=-50$ meV, (c) $V_B=-100$ meV, and (d) $V_B=-150$ meV.

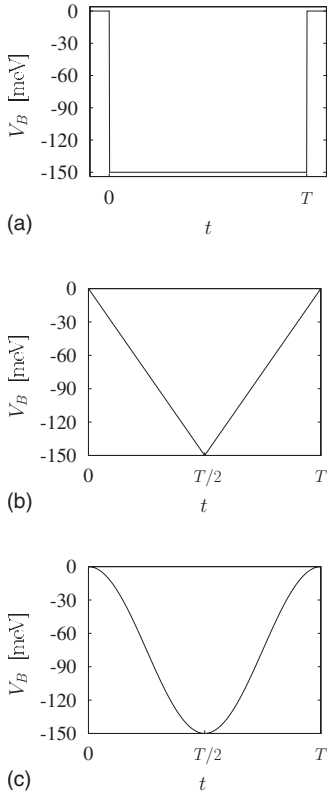

FIG. 2. Time dependence of top barrier energy V_B: (a) step function, (b) piece wise linear function, and (c) smooth (cosinus) function.

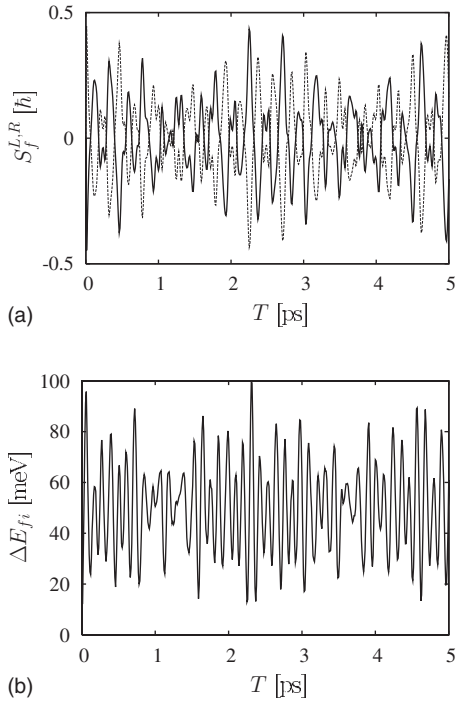

FIG. 3. (a) Expectation values $S_f^{L,R}$ of the z-spin component recorded at the end of the process of switching on and off the exchange interaction as a function of process duration time T for step like changes of the barrier. The solid (dashed) curve shows the results for an electron in the right (left) QD. (b) Energy difference ΔE_{fi} between the final- and initial-state energies as a function of process duration time T.

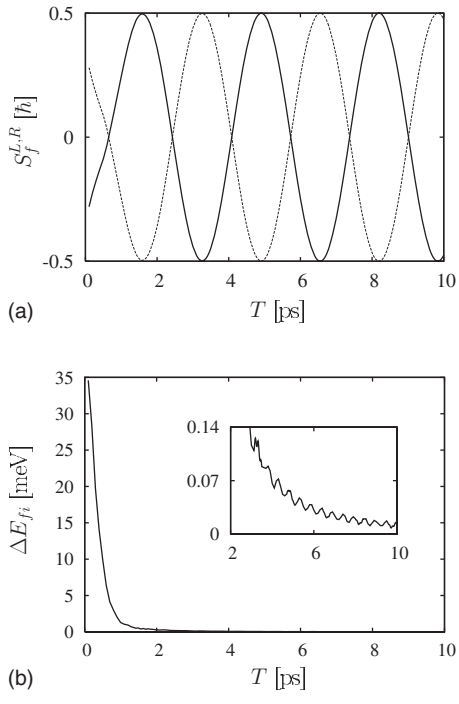

FIG. 4. (a) Expectation values $S_f^{L,R}$ of the z-spin component detected at the end of the process of switching on and off the exchange interaction as a function of duration time T for linear changes of the potential barrier. The solid (dashed) curve shows the results for the electron in the right (left) QD. (b) Energy difference ΔE_{fi} between the final and initial states as a function of duration time T of the process. The inset zooms in on part of this figure.

A. Time changes of the potential barrier

First, we study the effect of the step dependence of the barrier height on time [Fig. 2(a)]. In this process, the barrier top energy is rapidly lowered from $V_B=0$ to $V_B=-150$ meV—i.e., to the energy of the potential well bottom. We let the system to evolve for time $t=T$, after which the barrier is rapidly raised to the starting value. We have performed a series of simulations for different operation times T. We record the z-spin component expectation values $S_{i,f}^{L,R}$ for the left (L) and right (R) QD at the initial (i) and final (f) time instants.

The results, displayed in in Fig. 3(a), show that the spin expectation values $S_f^{L,R}$ rapidly oscillate as a function of time T and the amplitude of these oscillations does not reach $\hbar/2$. This means that sudden changes of the barrier do not lead to a full interchange of spins at any time interval T studied. The behavior of the energy difference $\Delta E_{fi}=E_f-E_i$ between the final and initial states [Fig. 3(b)] allows us to explain this effect. Similarly to the average electron spin, the energy difference ΔE_{fi} exhibits rapid oscillations as a function of process duration time T. We interpret the results of Fig. 3(b) as follows: during the sudden jumps of the barrier height the electron system is excited to higher-energy states. As a consequence, the energy of electrons in the final state increases; i.e., ΔE_{fi} is always larger than zero and exhibits jumps. Moreover, the electron wave function spreads out over the two potential wells. Therefore, the switching of the interaction between the electrons in a rapid manner does not lead to the required full swap of spins.

Next, we study the two-step process, during which the potential barrier height is a piece wise linear function of time [Fig. 2(b)]. In the first step, for $0\leq t\leq T/2$, the barrier height is lowered according to

$$V_B(t) = V_B^{max} - 2(V_B^{max} - V_B^{min})\frac{t}{T}, \tag{12}$$

where V_B^{max} (V_B^{min}) denotes the largest (smallest) barrier height reached during time interval T. In the second step—i.e., for $T/2\leq t\leq T$—the potential barrier is raised according to

$$V_B(t) = V_B^{min} + 2(V_B^{max} - V_B^{min})\left(\frac{t}{T} - \frac{1}{2}\right). \tag{13}$$

The results (Fig. 4) show that spin expectation values $S_f^{L,R}$ are oscillating functions of time with period T. Each extremal value $S_f^R=\pm\hbar/2$ of the z-spin component corresponds to the state, in which each electron possesses a spin orientation opposite to that in the initial state. Therefore, there exists a series of well-defined time intervals $T=T_n^{\pi}$, for which the z-spin component of each electron changes its sign. This means that both electrons interchange their spins: i.e., we deal with the spin swap operation. The subsequent extrema in Fig. 4(a) correspond to the π pulses with duration time

given by $T_n^{\pi}=nT_1^{\pi}+\text{const}$, where $n=1,2,\ldots$ numerates the subsequent extrema. If we increase the process duration time T, we simultaneously increase the time interval during which both electrons are localized in the same region of space. As a consequence, for the sufficiently long time T spin swapping can occur many times. If the process lasted for infinitely long time, the spin interchange would occur infinitely many times. This scenario would be realized for an isolated system (non interacting with an environment). In this case, spin expectation values $S_f^{L,R}$ would oscillate with amplitude $\hbar/2$ infinitely many times; i.e., there exists an infinite series of time intervals T_n^{π}, for which the spins are fully interchanged. However, in real systems, we deal with the decay of quantum states, which leads to the energy dissipation and the decoherence, which randomly changes the relative phase of spin qubits. These processes will lead to a decreasing amplitude of $S_f^{L,R}$ for increasing time interval T. Therefore, in order to perform a successful quantum logic operation the spin-swapping process should last for a possibly short time. However, there exists the lower limit on time interval T, during which the potential barrier is changed. This limit results from the requirement of adiabaticity of the process: the barrier has to be changed sufficiently slowly—i.e., in an adiabatic manner—in order to leave the system in the ground state. If the time interval T is too short, the system can undergo transitions to excited states, which leads to increase of energy and nonadiabaticity of the process.

The nonadiabaticity of the spin interchange process can be also observed in the behavior of $S_f^{L,R}(T)$ [Fig. 4(a)]. A closer look at the present computational results has led us to the observation that the first maximum is slightly lower than the other maxima. For the first maximum the exact spin expectation value reaches $\hbar/2$ with accuracy 98.7%. Similarly, due to spin conservation, for the first minimum, S_f^L reaches the value $-\hbar/2$ with the same accuracy. The extrema, which correspond to the second π pulse, reach $\pm\hbar/2$ with accuracy 99.4%. However, the next extrema of $S_f^{L,R}$ are equal to $\pm\hbar/2$ with a high precision. Therefore, we deal with several processes of incomplete interchange of spins before $S_f^{L,R}$ start to switch between values $\pm\hbar/2$. The lowering of the amplitude of $S_f^{L,R}$ is more pronounced if the process of changing the potential barrier is more rapid. The present results show that several processes of incomplete spin swapping can occur before we achieve a full interchange of spins, which leads to an elongation of the spin-exchange time. We note that this effect is not expected within the model, based on the effective Heisenberg Hamiltonian. In this model, the exchange interaction between the electrons is described by the Hamiltonian $H(t)=J(t)\mathbf{S}_1\cdot\mathbf{S}_2$,where $J(t)$ is the exchange interaction energy and the spin operators $\mathbf{S}_j$ $(j=1,2)$ are expressed in terms of the corresponding Pauli matrices. Our estimates show that in real quantum systems the spin interchange time can be longer than that resulting from the Heisenberg model, which does not take into account details of the physical implementation of switching on and off the exchange interaction.

Figure 4(b) displays the dependence of the energy separation ΔE_{fi} on duration time T of the process. In the inset, we zoom in on this dependence for the narrower time interval,

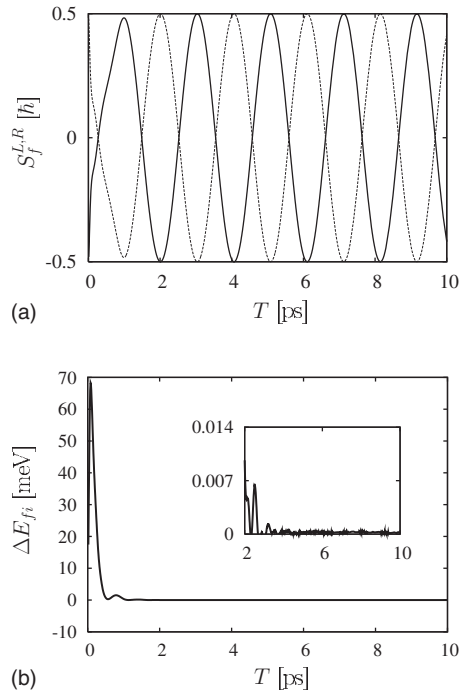

FIG. 5. (a) Expectation values $S_f^{L,R}$ of the z-spin component detected at the end of the process of switching on and off the exchange interaction as a function of process duration time T for smooth changes of the potential barrier. The solid (dashed) curve shows the results for the electron in the right (left) QD. (b) Energy difference ΔE_{fi} between the final and initial states as a function of duration time T of the process. The inset zooms in on part of this figure.

which allows us to observe the oscillations of ΔE_{fi}. The amplitude of these oscillations decreases with increasing T. Moreover, ΔE_{fi} asymptotically approaches zero for large T. In general, the positions of the local minima of ΔE_{fi} do not coincide with T_n^{π} [cf. Fig. 4(a)]. For the chosen nanostructure parameters, this coincidence appears for the third π pulse at $T=8.2$ ps. For piecewise linear changes of the potential barrier we deal with a sudden change of the confinement potential at $T/2$, which leads to the nonadiabaticity of this method of spin interchange.

Based on the above results, we expect that better results should be obtained if the potential barrier changes smoothly in time. Therefore, we have modeled the time dependence of the potential barrier by the following function [Fig. 2(c)]:

$$V_B(t)=\frac{1}{2}(V_B^{min}-V_B^{max})(1-\cos\omega t)+V_B^{max}, \qquad (14)$$

where $\omega=2\pi/T$. The results of simulations [Fig. 5(a)] show that the amplitude of $S_f^{L,R}(T)$ approaches $\hbar/2$ much faster than for linear changes of the potential barrier. Already the second maximum reaches $\hbar/2$ with accuracy 99.99%. Moreover, the results for the energy difference ΔE_{fi} [Fig. 5(b)] show that we can regard this process to be adiabatic for $T\geq 2$ ps. The amplitude of the periodic changes of $S_f^{L,R}$ remains constant (and equal to $\hbar/2$) for $T>2$ ps. The very fine

jumps of ΔE_{fi} near zero, which are visible in the inset of Fig. 5(b), result from the small numerical errors.

The spin of the single electron localized in the left (right) QD can be determined from Eq. (6) only if the probability of finding both electrons in the same QD is zero. This state is always prepared at the initial time instant and usually reached at the final instant in the process of potential barrier changes. At intermediate time instants, the electrons are not spatially separated; therefore, quantities $S^{L,R} \equiv S_z^{L,R}$, calculated from Eq. (6), are not equal to the eigenvalues of the z-spin component of the electron in the left and right QDs. Nevertheless, for arbitrary time t, $S^{L,R}$ can serve as spin-control indices.

In Fig. 6 we present the time dependence of the spin-control indices and energy of the two-electron system, which correspond to the pulses with duration times T_1^π and T_2^π for piecewise linear and smooth changes of the potential barrier. The energy is measured relative to the ground-state energy E_0 of two electrons in the lateral confinement potential ($E_0 = 2\hbar\omega_\perp$, where $\hbar\omega_\perp = 40$ meV). The behavior of these time characteristics is different for smooth and nonsmooth changes of the confinement potential. In the case of the nonsmooth process, the discontinuity of the first time derivative of the potential barrier energy for $t = T/2$ leads to a corresponding discontinuity of the energy versus time plot [cf. dotted curves in Figs. 6(a) and 6(b)]. The consequences of this discontinuity can also be seen in the time dependence of the spin-control indices [cf. solid and dashed curves in Figs. 6(a) and 6(b)]. For pulse with time duration $T_1^\pi = 1.6$ ps the spin indices begin to oscillate after reversing the time changes of the potential barrier [Fig. 6(a)]. The amplitude of these oscillations decreases with increasing potential barrier height and falls down to zero when the barrier height reaches the starting level. For the 3-times-longer pulse $T_2^\pi = 4.9$ ps, reversing the time changes of the potential barrier leads to smaller oscillations [cf. Fig. 6(b)]. Nevertheless, the time dependence of the spin control indices is still slightly perturbed.

In the case of smooth time changes of the barrier [Eq. (14)], the energy of the system is also a smooth function of time [Figs. 6(c) and 6(d)]. In spite of this, for the first π pulse with $T_1^\pi = 1.0$ ps the changes of the potential barrier are still seen by the electron system as rapid changes, which leads to a bending of the spin characteristics [Fig. 6(c)]. However, the time duration of the second π pulse ($T_2^\pi = 3.0$ ps) is sufficiently long so that the spin characteristics [Fig. 6(d)] stay smooth during the full process of switching on and off the exchange interaction. In the cases of linear and smooth changes of the potential barrier, the time evolution of spin indices $S^{L,R}(t)$ for the second π pulse with time duration T_2^π suggests that the full interchange of spins occurs as a result of manyfold exchange of spins between the electrons. For the second pulse the curves $S^{L,R}(t)$ go through zero 3 times [cf. Figs. 6(b) and 6(d)]. Thus, we conclude that in these processes we are dealing with a threefold incomplete swapping of spins before we finally obtain a full interchange of spin orientations. In order to obtain additional support for the occurrence of this process, we have observed the time changes of the second and third components of the total wave function [Eq. (3)]. The results of the simulations performed show the manyfold interchange of the second and third wave function components, which means that, in fact, the spins of the electrons change many times.

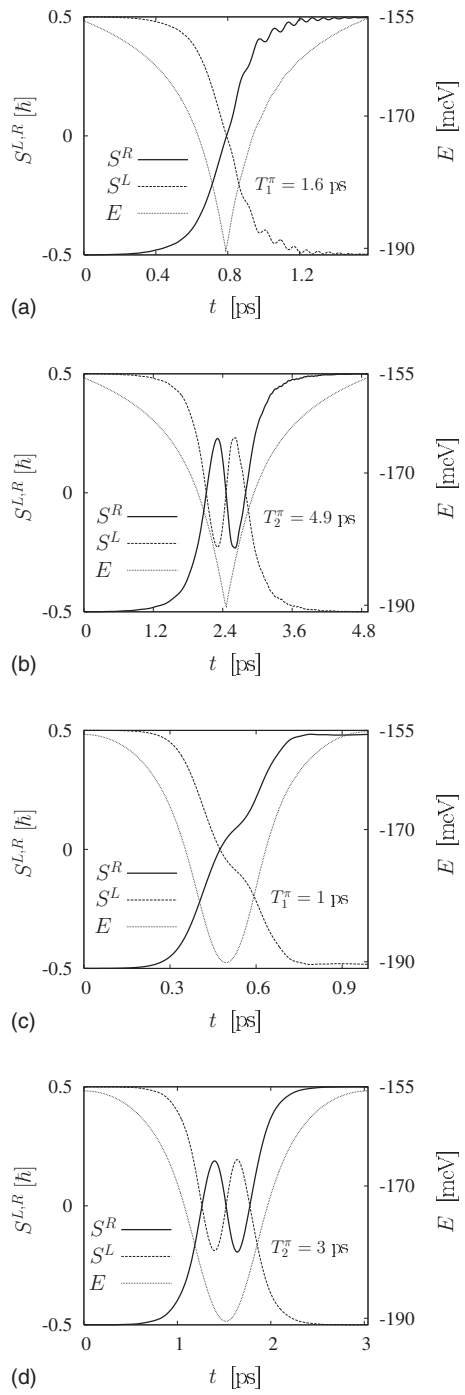

FIG. 6. Spin-control indices $S^{L,R}$ and energy E of the two-electron system as functions of time t. Plots (a) and (b) [(c) and (d)] correspond to the piecewise linear [smooth] changes of the potential barrier, and plots (a) and (c) [(b) and (d)] correspond to the first [second] π pulse with duration time T_1^π [T_2^π]. Solid (dashed) curves display the control spin index of the electron in the right (left) QD and the dotted curves show the energy of the system.

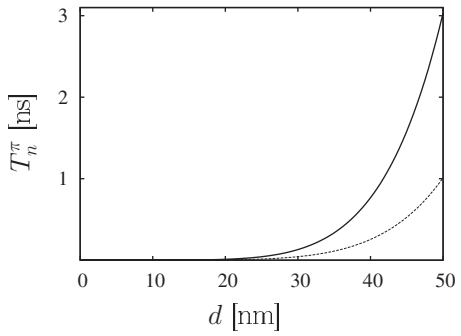

FIG. 7. Time duration T_n^π of the first ($n=1$, dotted curve) and second ($n=2$, solid curve) π pulses as a function of width d of the potential well.

Based on these results, we have chosen to further study the method of the smooth time dependence of the confinement potential [Eq. (14)], which seems to be the most promising for the manipulation with spin qubits.

B. Effect of quantum dot size and potential-well width asymmetry

If the size of the coupled QD nanostructure is sufficiently large, the Coulomb interelectron repulsion leads to a localization of electrons at the opposite potential well boundaries; i.e., the electrons form a Wigner molecule [33]. In the case of Wigner localization, the lowering of the potential barrier can cause no interchange of spins during a time which is shorter than the spin coherence time. We have checked the possibility of the occurrence of this effect by investigating the influence of the QD size of the time duration of the spin interchange process. The calculations have been performed for the QD nanostructure modeled by two rectangular potential wells separated by a potential barrier. The barrier thickness is fixed as $d_B=10$ nm, the potential barrier height is changed according to Eq. (14), the depths of both potential wells are equal ($V_L=V_R=-150$ meV), and the widths of both potential wells are also the same $d_L=d_R=d$. We change the potential well width in the interval 6 nm$\leq d\leq$50 nm. The spins are interchanged in the region of size $2d+d_B$. Figure 7 depicts the calculated time duration of the first and second π pulses as a function of potential well width d. We see that the time duration of the spin-swap operation quickly increases with increasing QD size. The size dependence of the duration time of the π pulses can be parametrized as follows: $T_n^\pi \sim d^6$. These results show that even for a QD with size as small as $d\simeq 50$ nm the spin-swap time can exceed the coherence time. Figure 7 also shows that, due to the rapid increase of T_n^π, the time interval between the subsequent π pulses quickly increases with increasing d.

In the Heisenberg model of the electron-electron interaction, the rate of spin interchange is determined by the exchange coupling constant, which is defined as the energy difference between the triplet and singlet states—i.e., $J=E_T-E_S$. For two identical QDs separated by a sufficiently thick and high potential barrier the triplet and singlet states are degenerate and $J=0$. If the potential barrier becomes thinner and lower, the wave functions of the electrons localized in both QDs start to overlap and the energies of triplet and singlet states become different, i.e.—$J\neq 0$. The coupling constant J can also be changed if the QD potential wells are different—i.e., if the QDs are asymmetric [34]. The larger the asymmetry of the potential wells, the larger the coupling constant. Therefore, one could expect that the asymmetry of the QDs should lead to a shortening of the spin interchange time. However, it turns out that this is not always the case [35].

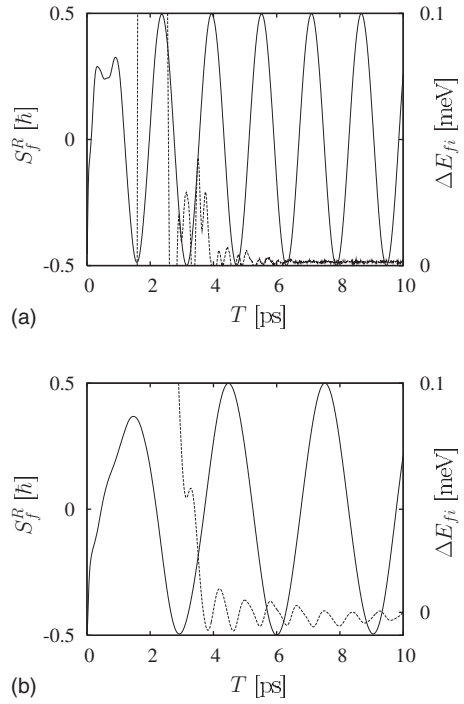

FIG. 8. Expectation value S_f^R of the z-spin component detected in the right QD at the end of the process of switching on and off the exchange interaction (solid curves) and energy difference ΔE_{fi} between the final and initial states (dashed curves) as functions of duration time T of spin interchange for asymmetric QDs. The width of the left QD is fixed $d_L=10$ nm, while the width of the right QD $d_R=5$ nm (a) and $d_R=15$ nm (b).

We have investigated the influence of the difference of the potential well widths on the duration time of spin interchange. For a fixed width of the left QD ($d_L=10$ nm) we have performed calculations for several values of width d_R of the right QD, changing the potential barrier according to Eq. (14). The results are displayed in Fig. 8 for $d_R=5$ nm and $d_R=15$ nm. For the sake of clarity, we present in Fig. 8 only the results for an electron in the right QD. Due to conservation of the total spin, the spin expectation values (S_f^L) for the electron in the left QD can be obtained by the reflection of $S_f^R(T)$ curves with respect to the axis $S_f^R=0$. If the right potential well is thinner than the left one, the energy difference ΔE_{fi} between the final and initial states tends to zero for a long duration time T of spin interchange [dashed curves in Fig. 8(a)]. However, if the right QD is thicker than the left one, ΔE_{fi} does not reach zero even for long time T [Fig. 8(b)]. Moreover, it takes on negative values for some time

intervals T. The negative values of ΔE_{fi} can be explained by a shift of the electron density toward a wider QD, in which the final-state energy is lower. Analyzing the plots of S_f^R vs T we have observed that the accuracy of the interchange of spins reaches 99.9%, but is never equal to 100%. We conclude that the asymmetry of the QD-confining potential results in an increasing multiplicity of spin interchange, which leads to a longer spin-swap duration time.

V. LATERALLY COUPLED QUANTUM DOTS

Electrostatic QDs with lateral interdot coupling have been the subject of many recent studies [6,37,36]. In laterally coupled QDs, the profile of the confinement potential can be modified by varying the voltages applied to the gates. This provides a convenient way of tuning the potential barriers and wells. However, due to technological limitations, the sizes of the lateral QDs, fabricated nowadays, are of the order of 100 nm [14], which makes them about 10 times larger than the size of the vertical QD [32] measured in the growth direction. The entire nanostructure consisting of two laterally coupled QDs separated by a potential barrier has a typical linear size 200–300 nm [38]. Due to this relatively large size, the duration time of the spin rotation is expected to be long (cf. see Sec. V B).

For lateral QDs we still apply the theoretical model described in Sec. II with the frozen transverse motion of electrons. Now (y,z) are transverse electron coordinates and we assume that the electrons move in the x direction. For example, the x axis can be directed along the effectively one-dimensional flow of electrons between the two lateral QDs [14]. The larger size of lateral QDs in comparison to that of vertical QDs leads to weaker electron localization and a weaker electron-electron interaction. According to Ref. [26] the strength of the potential confining the electrons in the transverse directions determines the strength of the effective electron-electron repulsion [Eq. (1)]. (We note that now V_{eff} is a function of x.) The excitation energy $\hbar\omega_\perp$ is a measure of the strength of the transverse parabolic confinement. In the calculations for lateral QDs, we take $\hbar\omega_\perp=5$ meV. Then, the transverse confinement potential rather well approximates the confinement in the double lateral QD fabricated in the TU Delft laboratory [38]. The present model is also applicable to quantum wires, which are composed from different semiconductors—e.g., InP and InAs [39]—which form a confinement potential profile of potential wells and barriers. In this case, we deal with stricktly quasi-one-dimensional coupled QDs. In the present section, we modify the exchange interaction between the electrons localized in laterally coupled QDs by tuning the potential barrier, which leads to simultaneous changes of the potential wells.

A. Symmetric quantum dots

The profile of the confinement potential for laterally coupled symmetric QDs is assumed in the form (Fig. 9)

$$V(x,t) = kx^2 + V_2(t)\exp[-(x-x_0)^2/d^2], \qquad (15)$$

where k determines the strength of the parabolic confinement potential, $V_2(t)$ can be interpreted as the potential barrier height for $V_2(t)>0$ and the potential well depth for $V_2(t)<0$, x_0 is the position of the center of the potential barrier (well), and d is the range of the Gaussian potential.

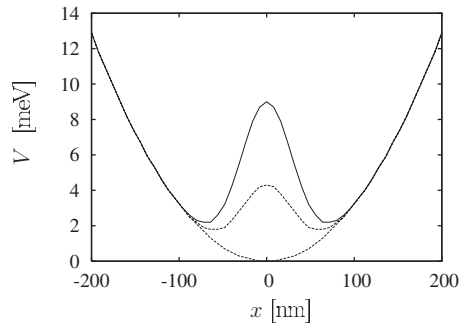

FIG. 9. Profiles of the confinement potential V vs x coordinate for two laterally coupled QDs for $V_2 \geq 0$. Parameters of the confinement potential [Eq. (15)] are $k=3.2\times10^{-4}$ meV $(\text{nm})^{-2}$, $d=42.5$ nm, $x_0=0$, $V_2=9.0$, 4.3, and 0 meV (from top to bottom).

The potential barrier separating the two QDs can be modified by changing $V_2(t)$ in the regime $V_2(t)\geq 0$. In the calculations, $V_2(t)$ was changed in time in a smooth manner—i.e., according to Eq. (14)—from 9 meV to 0 and back from 0 to 9 meV. Figure 9 shows the confinement potential profiles for the selected time instants. We see that changing the potential barrier we simultaneously change the potential wells. If the potential barrier is lowered, the electrons become localized closer to each other. We define the effective QD size $(d_{L,R}^{eff})$ as the width of the corresponding potential well determined at half the barrier height. At the initial time moment, the effective size of the QDs $d_L^{eff}=d_R^{eff}=100$ nm, the effective thickness of the barrier $d_B^{eff}=60$ nm, and the electron in the left (right) QD has spin $+\hbar/2$ $(-\hbar/2)$.

In Fig. 10, we display the time evolution of spin indices $S^{L,R}$ and energy V_2. We see that, in this case, the spin interchange occurs with 100% accuracy for the first π pulse with time duration $T_1^\pi=492$ ps. We also observe that, during the large part of the time evolution, the spins do not change. The spins start to rotate when the potential barrier height V_2 falls down below 5 meV. This suggests that the lowering of the initial height of the potential barrier should lead to a shorter spin rotation time. If the initial barrier height decreases, the

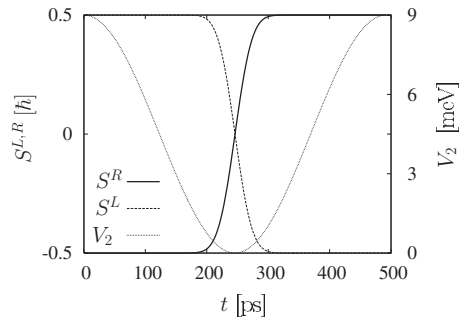

FIG. 10. Spin-control indices S^R for the right QD (solid curve) and S^L for the left QD (dashed curve) and potential barrier height V_2 (dotted curve) as functions of time t for duration time $T_1^\pi=492$ ps of the first π pulse.

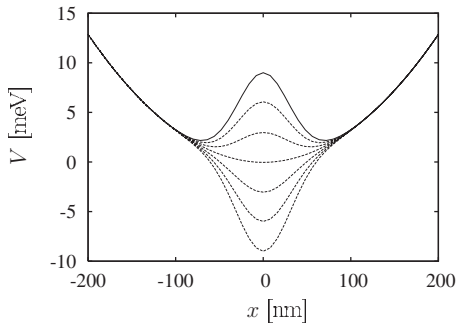

FIG. 11. Profile of the confinement potential V [Eq. (15)] as a function of coordinate x. Shown are the plots for $V_2=9,6,3,0,-3,-6,-9$ meV (from top to bottom). At the initial time instant (solid curve), $V_2=9$ meV, $d_B^{eff}=60$ nm, and $d_L^{eff}=d_R^{eff}=100$ nm.

effective QD size decreases too. This means that the shortening of the spin rotation time results from the size effect, discussed in Sec. IV B. For $V_2=5$ meV the effective size of the potential wells and the barrier decrease to $d_{L,R}^{eff}=76$ nm and $d_B^{eff}=42$ nm.

The fastest rate of spin interchange is observed for $V_2<1.5$ meV. Then, the effective QD sizes are $d_{L,R}^{eff}=40$ nm and $d_B^{eff}=42$ nm.

If the QD size is of the order of several tens of nanometers, the electrons are spatially separated even in the absence of a potential barrier [33]. For QDs of this size the Coulomb repulsion is sufficiently strong so that the electrons are localized in the QD boundaries and form Wigner molecules [33]. In order to achieve spin swapping the spatial wave functions of both electrons have to overlap. The larger the overlap, the faster the spin-swap operation. In the model nanostructure (Fig. 9), the effective size of the potential barrier is much smaller than that of the double potential well. Therefore, we can force the electrons to be localized in the same region of the nanostructure if we allow the parameter V_2 in Eq. (15) to take on a negative values during the time evolution. As a result, the potential barrier converts into a potential well (Fig. 11) and the electrons become localized in the same space region for some time during the changes of the confinement potential.

In the first computer run, the parameter V_2 has been changed in a smooth manner from 9 meV to −3 meV. As expected, we have obtained a considerably shorter duration time of the spin rotation; namely, the first π pulse lasted merely for 46.1 ps—i.e., it was more than 10 times shorter than in the previous case when we only turned off the potential barrier. A question appears: to what extent can we shorten the duration time of spin rotation by lowering the potential well bottom? In order to answer this question, we have performed a series of simulations, in which the minimum value V_2^{min} of the parameter V_2 was lowered from 0 to −9 meV. In each simulation, the initial value of the parameter V_2 was the same: $V_2(t=0)=V_2^{max}=9$ meV. The results are shown in Fig. 12. According to our expectation, the spin-swap duration time becomes shorter if V_2^{min} decreases. However, we also observe an undesirable effect; namely; the process ceases to be adiabatic, which results from the increasing amplitude of the changes of V_2 for a given process duration

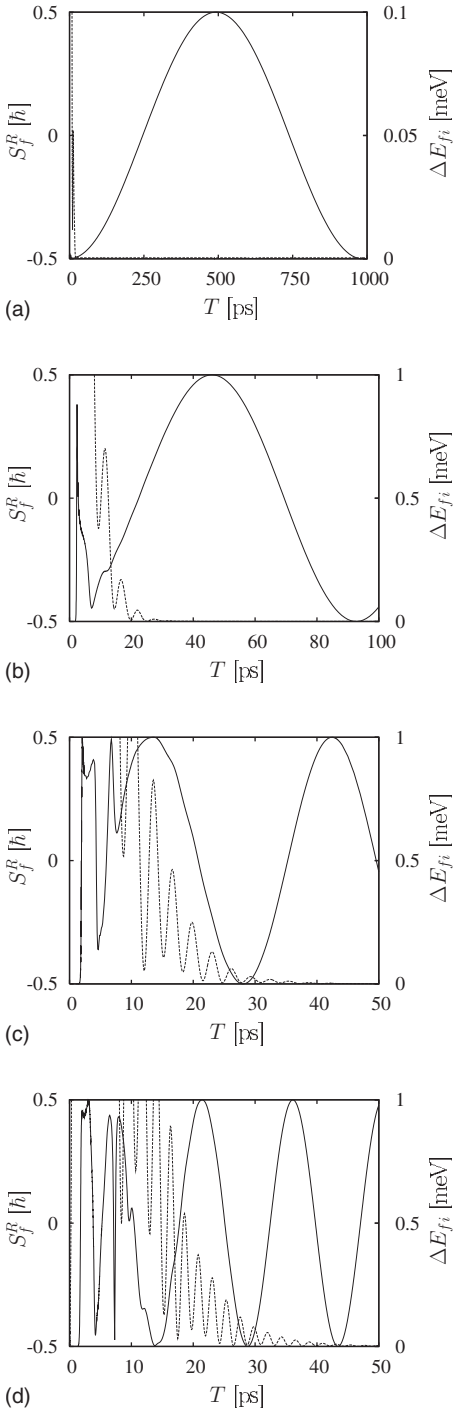

FIG. 12. Expectation value S_f^R of the z-spin component in the right QD (solid curve) and energy difference ΔE_{fi} (dashed curve) between the final and initial states as a function of time duration T of the process. (a) $V_2^{min}=0$, (b) $V_2^{min}=-3$ meV, (c) $V_2^{min}=-6$ meV, (d) $V_2^{min}=-9$ meV.

time T. The nonadiabaticity is visible in Figs. 12(a)–12(d) as oscillations of the energy difference $\Delta E_{fi}(T)$ and deformations of plots $S_f^R(T)$ for small T. For $V_2^{min}=0$ the process can be treated as adiabatic if $T\geq 25$ ps, whereas for $V_2^{min}=-9$ meV the adiabaticity is reached if $T\geq 55$ ps. We conclude that the lowering of V_2^{min} below −3 meV is not

advantageous. The shortest time of the full interchange of spins has been obtained for $V_2^{min}=-3$ meV. In this case, the orientation of spins was changed in a single swap after time $T_1^{\pi}=46.1$ ps with accuracy 100%.

We note that for laterally coupled QDs the conversion of the potential barrier into a potential well means that a section of quantum wire is formed below the gate electrodes, which create the confinement potential in the electrostatic QDs [38]. However, in this process, the spin qubits can be destroyed if the electrons will tunnel from the two-dimensional electron gas [38] to the QD. Therefore, it seems that the mechanism of conversion of the interdot potential barrier into the potential well will not lead to the required rotation of spins in laterally coupled QDs. However, this mechanism can be applicable to the spin qubits in vertically coupled QDs [31] and the coupled QDs formed in quantum wires [39].

B. Asymmetric quantum dots

The bias voltage applied to coupled QDs leads to an asymmetry of the confinement potential profile; i.e., the potential well depths become different. This suggests another mechanism of swapping the spins, which can be modeled by raising and lowering the bottom of one potential well. Raising the potential well bottom of one QD will stimulate the flow of the electron to the second QD. Finally, both electrons will be localized in the same QD. The subsequent lowering of the potential well bottom back to the initial level will force the flow of one of the electrons to the first QD. We expect that a suitable adjustment of the potential well should cause the desired electron spin swapping. This mechanism is advantageous since, according to the results of Sec. IV B, a stronger electron localization leads to a shorter spin-swapping time.

In order to simulate this process, we model the confinement potential by the linear combination of two Gaussians—i.e.,

$$V(x,t) = V_1 \exp[-(x-x_1)^2/d_1^2] + V_2(t)\exp[-(x-x_2)^2/d_2^2], \tag{16}$$

where V_1 and $V_2(t)$ are the potential well depths, x_1 and x_2 are the positions of the centers of the QDs, and d_1 and d_2 determine the sizes of the QDs (Fig. 13). In Eq. (16), indices 1 and 2 correspond to the left and right QD, respectively.

We fix V_1 and tune the potential well depth of the right QD by changing $V_2(t)$ according to the smooth function of time [Eq. (14)]. As in the previous simulations, the electron in the right (left) QD has spin $+\hbar/2$ $(-\hbar/2)$ at the initial time instant. We have performed several simulations for different time intervals T with the other parameters of the confinement potential [Eq. (16)] being fixed—namely, $V_1=-10$ meV, $d_1=d_2=64$ nm, and $x_2=-x_1=58$ nm. For $t=0$ (solid curve in Fig. 13) the bottom of both potential wells is at the level $V=-10.4$ meV, $d_1=d_2=48$ nm, $d_B=51$ nm, and the relative height of the potential barrier is 1.7 meV. In each computer run, the initial (minimal) value of the parameter V_2 is set to $V_2(t=0)=V_2^{min}=-10$ meV. The potential profiles shown in Fig. 13 suggest that it is not necessary to remove the right QD potential well entirely in order to localize both electrons in the left QD. Again, we are looking for an answer to the question, for which range of changes of the potential well bottom of the right QD is the spin-swap duration time the shortest? The results of the simulations are displayed in Fig. 14. As in previous figures, for the sake of clarity, we present only the spin expectation values S_f^R for the right QD, since S_f^L can be obtained from the spin conservation principle. If the parameter V_2 is changed from $V_2^{min}=-10$ meV to $V_2^{max}=0$, the amplitude of changes of the right QD potential well bottom is so large that even for $T\simeq 100$ ps the spin interchange process is nonadiabatic. In this case, we observe the spin swapping with accuracy 99.8% for $T^{\pi}\simeq 200$ ps. The process of a full interchange of spins becomes adiabatic for T of the order of several hundred picoseconds. Therefore, the process, during which one of the potential wells is entirely removed, is not advantageous. In order to remove this disadvantage, we reduce the amplitude of changes of parameter V_2 by decreasing the maximum value V_2^{max}. Useful results are obtained when raising the potential well bottom to $V_2^{max}=-3$ meV [Fig. 14(a)]. The shortest π pulse time $(T_1^{\pi}=127$ ps) has been obtained for $V_2^{max}=-6.1$ meV [Fig. 14(c)]. In this case, the process is adiabatic for $T>100$ ps. Similarly as for symmetric QDs, there exists an optimal regime of changes of the parameter V_2, in which the spin-swap time is minimal and the process is adiabatic. We note that the parameter V_2^{max} cannot be too small since then the potential well bottom is not raised high enough and the tunneling probability of the electron from the right to left QD is too small, which leads to a long spin-swap duration time. For example, for $V_2^{max}=-7$ meV, $T_1^{\pi}=713$ ps.

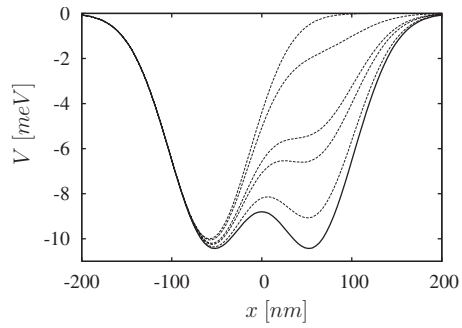

FIG. 13. Profile of the confinement potential V [Eq. (16)] as a function of coordinate x for several time instants. The parameter $V_1=-10$ meV is fixed. At the initial moment, $V_2(t=0)=-10$ meV (solid curve). Shown are also the potential profiles for $V_2=-7$, -6.1, -5, -3, and 0 meV (from bottom to top).

We conclude that the time changes of the confinement potential, which lead to asymmetry of QDs, result in a considerable shortening of the spin-swap time if the amplitude of potential well changes is of the order of ~ 5 meV.

VI. DISCUSSION

Coherent control of electron spin states in coupled QDs was demonstrated experimentally by Petta *et al.* [18]. The authors [18] showed that a suitable change of gate voltages

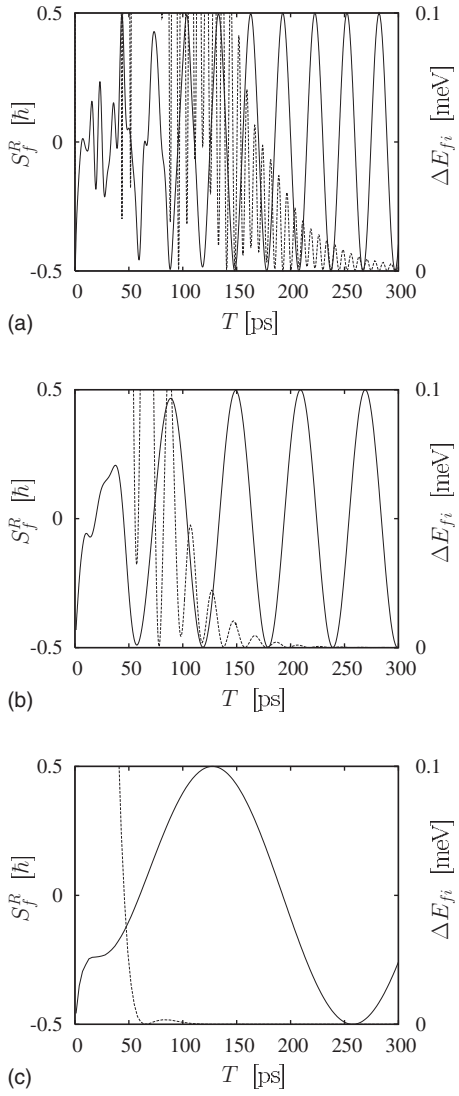

FIG. 14. Expectation value S_f^R (solid curve) of the z-spin component of the electron in the right QD and energy difference ΔE_{fi} (dotted curve) as functions of duration time T of potential changes for asymmetric QDs. (a) $V_2^{max}=-3$ meV, (b) $V_2^{max}=-5$ meV, and (c) $V_2^{max}=-6.1$ meV.

allows for control of exchange interaction and coherent manipulation of two-electron spin states. This paper provides a good starting point for an implementation of coupled QDs to solid-state-based quantum computation.

When using the controlled exchange interaction to manipulate with electron spins in coupled QDS, we are dealing with the double-electron occupancy problem [17], which leads to possible quantum computation errors. Schliemann *et al.* [17] studied this problem using the Hund-Mulliken molecular-orbital method with six-element basis. The authors [17] calculated the time-dependent transitions between the spin-swapped initial and final two-electron states and, for the assumed smooth time dependence of the tunneling amplitude, obtained adiabatic transitions between stationary states. We note that the present approach allows us to simulate a temporal evolution of the system in a complete basis in space-coordinate representation. Therefore, we take into account the dependence of the two-electron wave function on the varying confinement potential; i.e., we can directly observe the changes of QD occupancy that lead to a switching on and off of the exchange interaction. In order to illustrate the effect of the QD occupancy, we have calculated the one-electron probability density $\rho(x,t)$ by integrating the two-electron probability density $\rho(x_1,x_2,t)=|\psi(x_1,x_2,t)|^2$ over the coordinate x_2 [cf. Eq. (14) in Ref. [28]]. The results are presented in Figs. 15(a) and 15(b) as functions of time and one-electron coordinate $x=x_1$. Figure 15(a) corresponds to the second peak in Fig. 14(b), for which $T_2^\pi=88.8$ ps and $S_f^R(T_2^\pi)=0.93\times(\hbar/2)$, while Fig. 15(b) corresponds to the fifth peak in Fig. 14(b), for which $T_5^\pi=269$ ps and $S_f^R(T_5^\pi)=0.99\times\hbar/2$. The results of Figs. 15(a) and 15(b) can be interpreted as follows: at the initial time instant, both electrons are localized in different QDs, but after raising the potential well bottom of the right QD, the electron, initially localized in the right QD, tunnels to the left QD, which leads to a double occupancy of the left QD. Next, the potential well bottom of the right QD is lowered, which causes one of the electrons to tunnel back to the right QD. The electron densities in Figs. 15(a) and 15(b) considerably differ between each other. In case (a), in the doubly occupied QD, the electron probability density oscillates in time, which demonstrates that the electrons are in nonstationary states—i.e., can occupy both the ground and excited states. The electrons are not in the energy eigenstates, since the changes of the confinement potential are too fast. These oscillations of the electron density are still present in the final state—i.e., after separation of the electrons. Figure 15(b) corresponds to the

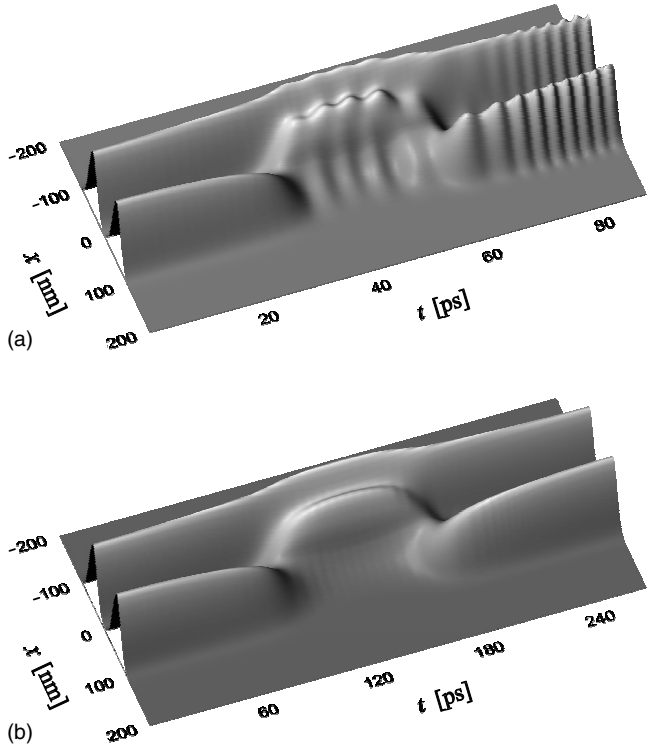

FIG. 15. One-electron probability density $\rho(x,t)$ as a function of coordinate x and time t. Part (a) corresponds to the second peak on Fig. 14(b), part (b) corresponds to the fifth peak on Fig. 14(b).

adiabatic process [cf. Fig. 14(b) for $T>250$ ps], during which the electrons are in the ground state of the time-dependent Hamiltonian. In case (b), the electron probability density changes smoothly in time and does not exhibit oscillations. The results of Fig. 15(b) are in qualitative agreement with those of Schliemann *et al.* [17], who considered smooth time changes of the tunneling amplitude.

We have studied the processes with different rates of time changes of the confinement potential. We have shown that the spin-swap operation in the coupled QDs can be more complicated than that resulting from the simple Heisenberg model. In particular, sudden changes of the confinement potential can lead to nonadiabatic processes, during which the quantum information stored in the spin qubits is destroyed.

VII. CONCLUSIONS AND SUMMARY

In the present paper, we have proposed a method for a theoretical quantitative description of the spin-swapping process in a double QD. Using this method we have estimated the spin-swap duration time induced by the exchange interaction between electrons in vertically and laterally coupled QDs. The results obtained are also valid for quantum wires, which contain coupled QDs. The process of switching on and off the exchange interaction, considered in the present paper, is triggered by the corresponding time changes of the confinement potential profile. The time dependence of the confinement potential is of crucial importance for the efficiency of the spin interchange. We have shown that the confinement potential should change smoothly and sufficiently slowly in time to ensure the adiabaticity of the spin-swap operation.

We have also shown that full spin interchange (with 100% accuracy) can hardly be achieved in a single-step spin-swap process. In the coupled QD system, full spin interchange occurs, in general, as a result of many steps of incomplete spin swaps. The most promising results—i.e., the shortest time of full spin swapping in the adiabatic process—have been obtained when the shape of the potential in the interdot region has been changed according to the smooth function of time from the potential barrier to the potential well. However, it seems to be difficult to realize this process experimentally in the same nanodevice by merely changing the voltages applied to the gate electrodes, which define the laterally coupled QDs.

The results obtained for vertical asymmetric QDs with different widths of the potential wells (Sec. IV B) are rather disappointing: it turns out that this type of asymmetry of the confinement potential leads to an increase of the spin-swap duration time, since in this case a full spin swap is obtained after several incomplete spin swaps. However, in the case of asymmetry discussed in Sec. V B for the lateral QDs—i.e., different depths of the potential wells—we can always choose the range of changes of the QD parameters in order to obtain full spin swapping in a single step. In vertically and laterally coupled QDs the spin-swap duration time decreases if the range of the confinement potential becomes shorter. This leads to the conclusion that the size of the coupled QD system should be smaller than ~ 100 nm in order to obtain a sufficiently short spin swap time. We provide numerical estimates of the nanostructure parameters, for which the spin-swap operation is optimally performed.

One can consider the problem of scalability of the present two-electron coupled QD system. The scalable QD system might be realized, e.g., according to the proposal [4,40], as several QDs embedded in a microcavity and interacting with cavity modes.

In summary, the exchange interaction controlled by time changes of the confinement potential leads to a swapping of the electron spins and can serve as a mechanism to manipulate with spin qubits in coupled QDs. The spin-swap duration time, which is several orders of magnitude shorter than the spin-coherence time, can be obtained for coupled QDs of possibly small size, in which an alternate gate voltage induces the confinement potential, which changes sufficiently smoothly and slowly in time. Fabrication of nanodevices, which satisfy these requirements, is a challenging task for nanotechnology.

ACKNOWLEDGMENTS

We are grateful to Jason Petta for bringing to our attention the results of Ref. [18]. S. M. thanks to Professor Daniel Loss for fruitful scientific discussions during the Winter 2007 Aspen Condensed Matter Conference. This paper has been partly supported by the Polish Ministry of Science and Higher Education.

[1] D. P. DiVincenzo, Phys. Rev. A **51**, 1015 (1995).
[2] B. E. Kane, Nature (London) **393**, 133 (1998).
[3] D. Loss and D. P. DiVincenzo, Phys. Rev. A **57**, 120 (1998).
[4] A. Imamoglu, D. D. Awschalom, G. Burkard, D. P. DiVincenzo, D. Loss, M. Sherwin, and A. Small, Phys. Rev. Lett. **83**, 4204 (1999).
[5] R. Vrijen, E. Yablonovitch, K. Wang, H. W. Jiang, A. Balandin, V. Roychowdhury, T. Mor, and D. DiVincenzo, Phys. Rev. A **62**, 012306 (2000).
[6] H. A. Engel, P. Recher, and D. Loss, Solid State Commun. **119**, 229 (2001).
[7] J. Levy, Phys. Rev. A **64**, 052306 (2001).
[8] M. N. Leuenberger and D. Loss, Physica E (Amsterdam) **10**, 452 (2001).
[9] V. Privman, D. Mozyrsky, and I. D. Vagner, Comput. Phys. Commun. **146**, 331 (2002).
[10] M. Friesen, P. Rugheimer, D. E. Savage, M. G. Lagally, D. W. van de Weide, R. Joynt, and M. A. Eriksson, Phys. Rev. B **67**, 121301(R) (2003).
[11] A. M. Stoneham, A. J. Fisher, and P. T. Greenland, J. Phys.: Condens. Matter **15**, L447 (2003).
[12] M. Feng, Phys. Lett. A **306**, 353 (2003).
[13] H. A. Engel, L. P. Kouwenhoven, D. Loss, and C. M. Marcus, Quantum Inf. Comput. **3**, 115 (2004).

[14] J. M. Elzerman, R. Hanson, L. H. W. van Beveren, S. Tarucha, L. M. K. Vandersypen, and L. P. Kouwenhoven, Lect. Notes Phys. **667**, 25 (2005).
[15] D. P. DiVincenzo and D. Loss, Superlattices Microstruct. **23**, 419 (1998).
[16] G. Burkard, D. Loss, and D. P. DiVincenzo, Phys. Rev. B **59**, 2070 (1999).
[17] J. Schliemann, D. Loss, and A. H. MacDonald, Phys. Rev. B **63**, 085311 (2001).
[18] J. R. Petta, A. C. Johnson, J. M. Taylor, E. A. Laird, A. Yacoby, M. D. Lukin, C. M. Marcus, M. P. Hanson, and A. C. Gossard, Science **309**, 2180 (2005).
[19] T. Meunier, I. T. Vink, L. H. Willems van Beveren, F. H. L. Koppens, H. P. Tranitz, W. Wegscheider, L. P. Kouwenhoven, and L. M. K. Vandersypen, Phys. Rev. B **74**, 195303 (2006).
[20] R. Hanson, B. Witkamp, L. M. K. Vardersyoen, L. H. Willems van Beveren, J. M. Elzerman, and L. P. Kouwenhoven, Phys. Rev. Lett. **91**, 196802 (2003).
[21] H. Sasakura, S. Muto, and T. Ohshima, Physica E (Amsterdam) **10**, 458 (2001).
[22] Y. Wu, X. Li, D. Steel, D. Gammon, and L. J. Sham, IEEE Trans. Adv. Packag. **25**, 242 (2004).
[23] D. Loss and D. P. DiVincenzo, Phys. Rev. A **57**, 120 (1998).
[24] D. P. DiVincenzo, D. Bacon, J. Kempe, G. Burkard, and K. B. Whaley, Nature (London) **408**, 339 (2000).
[25] V. V. Dobrovitski, J. M. Taylor, and M. D. Lukin, Phys. Rev. B **73**, 245318 (2006).
[26] S. Bednarek, B. Szafran, T. Chwiej, and J. Adamowski, Phys. Rev. B **68**, 045328 (2003).
[27] K. T. R Davies, H. Flocard, S. Krieger, and M. S. Weiss, Nucl. Phys. A **342**, 111 (1980).
[28] S. Moskal, S. Bednarek, and J. Adamowski, Phys. Rev. A **71**, 062327 (2005).
[29] J. Preskill, Proc. R. Soc. London, Ser. A **454**, 385 (1998).
[30] J. M. Elzerman, R. Hanson, L. H. Willems van Beveren, B. Witkamp, L. M. K. Vandersypen, and L. P. Kouwenhoven, Nature (London) **430**, 431 (2004).
[31] D. G. Austing, S. Tarucha, H. Tamura, K. Muraki, F. Ancilotto, M. Barranco, A. Emperador, R. Mayol, and M. Pi, Phys. Rev. B **70**, 045324 (2004).
[32] S. Tarucha, D. G. Austing, and T. Honda, R. J. van der Hage, and L. P. Kouwenhoven, Phys. Rev. Lett. **77**, 3613 (1996).
[33] S. Bednarek, T. Chwiej, J. Adamowski, and B. Szafran, Phys. Rev. B **67**, 205316 (2003).
[34] B. Szafran, F. M. Peeters, and S. Bednarek, Phys. Rev. B **70**, 205318 (2004).
[35] B. Szafran, F. M. Peeters, and S. Bednarek, Phys. Rev. B **70**, 125310 (2004).
[36] A. M. Chang, Science **293**, 2221 (2001).
[37] N. C. van der Vaart, S. F. Godijn, Y. V. Nazarov, C. J. P. M. Harmans, J. E. Mooij, L. W. Molenkamp, and C. T. Foxon, Phys. Rev. Lett. **74**, 4702 (1995).
[38] J. M. Elzerman, R. Hanson, J. S. Greidanus, L. H. Willems van Beveren, S. De Franceschi, L. M. K. Vandersypen, S. Tarucha, and L. P. Kouwenhoven, Phys. Rev. B **67**, 161308(R) (2003).
[39] M. T. Bjőrk, B. J. Ohlsson, T. Sass, A. I. Persson, C. Thelander, M. H. Magnusson, K. Deppert, L. R. Wallengerg, and L. Samuelson, Appl. Phys. Lett. **80**, 1058 (2002).
[40] A. Miranowicz, S. K. Özdemir, Y. X. Liu, M. Koashi, N. Imoto, and Y. Hirayama, Phys. Rev. A **65**, 062321 (2002).